

Microstructure and mechanical properties of silicon nitride with tri-laminate structures

Dong-Soo Park^{a,*}, Tae-Wook Roh^b, Byung-Dong Han^a, Hai-Doo Kim^a, Chan Park^b

^a*Ceramic Materials Group, Korea Institute of Machinery and Materials, 66 Sang-Nam-Dong, Chang-Won, Kyong-Nam, South Korea*

^b*Department of Materials Science and Engineering, Pukyong National University, Pusan, South Korea*

Received 29 June 2000; received in revised form 29 March 2001; accepted 28 April 2001

Abstract

Silicon nitride ceramics with tri-laminate structures were prepared using two kinds of layers; layer with the aligned silicon nitride whisker seeds (named as “S” layer) and layer without the seed (“N” layer). The fracture toughness values on the casting surface of N layer of sample with a tri-laminate structure (N–S–N structure) showed an anisotropy, and this is contrary to the isotropic fracture toughness observed from the casting surface of sample consisting of only N layers. The fracture toughness anisotropy observed from N layer of the former sample is explained in terms of the microstructural anisotropy induced by the sintering shrinkage anisotropy within the casting plane. © 2002 Published by Elsevier Science Ltd.

Keywords: Anisotropy; Laminates; Seeding; Si₃N₄; Toughness

1. Introduction

Silicon nitride has been widely studied for structural applications. It has many good properties including high strength, high fracture toughness, and good thermal shock resistance. Its good properties are closely related to the microstructure that consists of large elongated grains, fine acicular matrix grains, and weak intergranular glassy phase. Those large elongated grains are needed for the improved fracture toughness, but they often deteriorate the flexural strength as reported by Lee et al.¹ One of the methods that can improve both the flexural strength and the fracture toughness takes advantage of alignment of those large elongated grains as reported by Hirao et al.² Alignment of the anisotropic grains that grow from the seeds has been considered as one of the methods for improving the properties of ceramics in a specific orientation.^{3,4} While most of those reports on ceramics with the aligned anisotropic seeds are concentrated on the large grains growing from the seeds,^{2–6} little attention has been paid to orientation of the “matrix grains”.

Another method for improving the properties of silicon nitride ceramics by controlling the microstructure is making a composite with a multiple layered structure. Lee et al. prepared a bi-layer silicon nitride composite consisting of a hard coating layer and a soft substrate, which can preserve both high wear resistance and high fracture toughness.⁷ A residual stress between the layers with different thermal expansion coefficients is also taken advantage of for improving the properties.^{8,9} A compressive residual stress on the surface can arrest the crack propagation as reported by Rao et al.⁸ Choi et al. were able to improve both the flexural strength and the fracture toughness of silicon nitride by making a three-layer composite that had a mid-layer with 20 vol.% SiC platelets.⁹ Moya et al. prepared multi-layer composites using different kinds of alumina–zirconia composite layers. They reported that the calculated compressive residual stress in the alumina–monoclinic zirconia layer was higher than 1 GPa.¹⁰ While most of the works dealing with a multi-layer composite have been concentrated on the effect of the residual stress on the properties, little attention has been paid to the microstructural change of the matrix grains that occurs during making the composite.

In this study, four kinds of silicon nitride samples are prepared by tape casting the slurry with and without the

* Corresponding author.

E-mail address: pds1590@kmail.kimm.re.kr (D.-S. Park).

silicon nitride whisker seeds and gas pressure sintering. Anisotropy of the microstructure within the layer without the whisker seed and the properties of sintered sample are explained in terms of the sintering shrinkage anisotropy.

2. Experimental

Slurry for tape casting was prepared from the ceramic powders, dispersant (Hypermer KD-1, ICI Chemical Co., Barcelona, Spain), binder [poly(vinylbutyral), Aldrich Chemical Co., Milwaukee, WI], plasticizer (dibutyl phthalate, Aldrich Chemical Co.), and solvent (methyl isobutyl ketone) by planetary ball mill. Details of the slurry composition is provided in the previous report.¹¹ Ceramic powder composition of N layer was 93 wt.% α -Si₃N₄ (Ube Industries Co., Ltd., Tokyo, Japan), 6 wt.% Y₂O₃ (Fine, H.C. Starck Co. & GmbH, Berlin, Germany) and 1 wt.% MgO (EP, Junsei Chemical Co., Tokyo, Japan). For S layer, the powder composition was 90 wt.% α -Si₃N₄, 3 wt.% of β -Si₃N₄ whiskers (SN-WB, Ube Industries), 6 wt.% Y₂O₃ and 1 wt.% MgO. After the casting, the tapes were dried overnight in open air. Then, they were cut and stacked. Four kinds of samples were prepared according to the stacking sequences; N, N-S-N, S-N-S, and S. Samples N and S consist of the same kind of sheets without the whisker and with the whiskers, respectively. Lamination was carried out at 353 K under 30 MPa for 0.5 h. Binder removal was performed at 623 K for 10 h, and then, samples were cold isostatically pressed under 250 MPa. Gas pressure sintering of samples was carried out at 2148 K for 4 h under 2 MPa nitrogen pressure. Samples N-S-N and S-N-S were prepared in such a way that thickness of the middle layer was about 2.5 mm after sintering. The linear sintering shrinkage values in three directions shown in

Fig. 1 were obtained by measuring the corresponding lengths of sample before and after sintering. Sintered density was measured by water immersion method. The elastic properties of N sample and S sample were measured by pulse echo overlap method using a high power ultrasonic analyzer (RAM5000, Ritec Inc., Warwick, RI, USA). Those properties of S sample were measured in two directions (parallel and normal to the alignment direction). The linear thermal expansion coefficients of N sample and S sample were measured in the temperature range between 298 and 1223 K in nitrogen. The dimensions of samples for the thermal expansion measurements were 3×4×20 mm, and the measurements were performed in the 20 mm direction. In the case of the S sample, the thermal expansion coefficients were measured in the two directions, parallel and normal to the alignment direction. As a reference, pure Tungsten was used for the thermal expansion measurements.

Samples were ground to 3.5 mm in thickness with a 400 grit diamond wheel, and then, they were cut into bars with dimensions of 4×3.5×25 mm. The largest four surfaces were machine polished with 1 μ m diamond slurry, and sample thickness was polished down to about 3 mm. A special attention was paid to polishing the samples with tri-laminate structures to have the top surface layers about 0.2 mm thick. Fig. 1 shows schematic diagrams of the four kinds of samples. After polishing, samples were heated to 1373 K for 2 h in a flowing nitrogen environment in order to relieve the residual stress that might be developed during cooling in the gas pressure sintering furnace. The three point flexural strength was measured using 20 mm span and cross-head speed of 0.5 mm/min. A special attention was paid to have the top surface subjected to tension. Five to eight strength values were measured from each kind of sample. Microvickers hardness under 9.8 N load was measured. Vickers indentations under 98 N load and 49

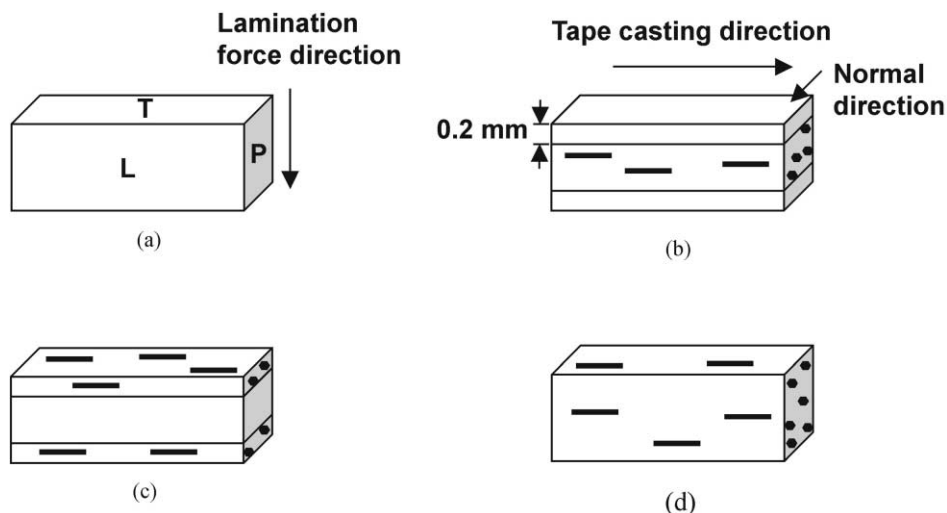


Fig. 1. Schematic diagram of samples used in this study; (a) sample N, (b) sample N-S-N, (c) sample S-N-S, and (d) sample S.

N load were performed on the top surface (surface T) and on the side surface parallel to the casting direction (surface L), respectively. Some of N–S–N samples were prepared to have very thick surface layers (about 0.5 mm) and indentation was carried out on surface L.

The microstructure of sample was examined using scanning electron microscope after plasma etching. Plasma etching was carried out with 95% CF_4 –5% O_2 gas mixture. Width and length of the largest 230 grains and 298 grains were measured from sample N and S, respectively using image analysis software (Image-Pro 3.0, Media Cybernetics, L.P., Silver Spring, MD, USA). Angles between the long axes of about 200 large elongated grains of each sample and the casting direction were measured, and distribution of the angles was also obtained.

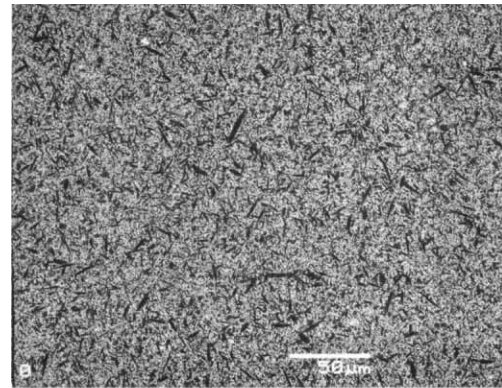
3. Results and discussion

3.1. Microstructure

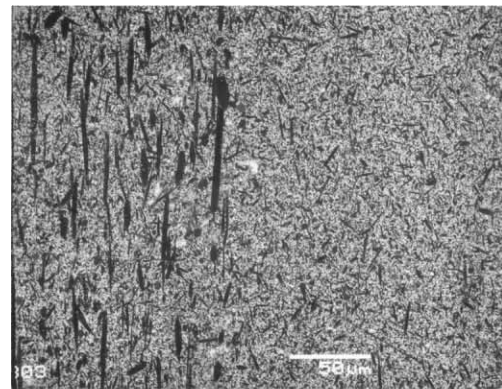
All the samples were sintered to higher than 99% theoretical. Fig. 2 shows SEM micrographs of samples N, S–N–S and S. Matrix grains of S layer are as fine as those of N layer. Table 1 shows the sizes and aspect ratios of the large grains in N sample and S sample. Average width and length of the largest 230 grains of sample N were 2.58 and 5.26 μm , respectively. It is difficult to obtain the real aspect ratio of the elongated grains of silicon nitride from SEM micrograph of the etched surface. According to Mitomo, the real aspect ratio is approximated by mean value of the 10% highest observed ratios.¹² Mean value of the 10% highest aspect ratios measured from sample N was 5.62. Average width and length of the largest 230 grains of sample S were 2.82 and 12.67 μm , respectively: Mean value of the 10% highest aspect ratios was 10.53. All the samples showed the shrinkage anisotropy during sintering as shown in Fig. 3. The sintering shrinkage in the lamination force direction is the biggest among those in the three directions. Sample S and the two tri-laminate samples also exhibited the shrinkage anisotropy within the casting plane: The shrinkage is smaller in the casting direction than in the direction normal to the casting direction. The in-plane shrinkage anisotropy of sample S is caused by presence of the aligned whisker seeds that originally have dimensions of 10.5 μm in length and 0.6 μm in

width on average.¹³ Those whiskers are single crystals and they do not have any pore to be removed during sintering. Highly anisotropic shape of the whisker seeds inhibits the shrinkage in the length direction and leads to the observed sintering shrinkage anisotropy as described in the previous report.¹³

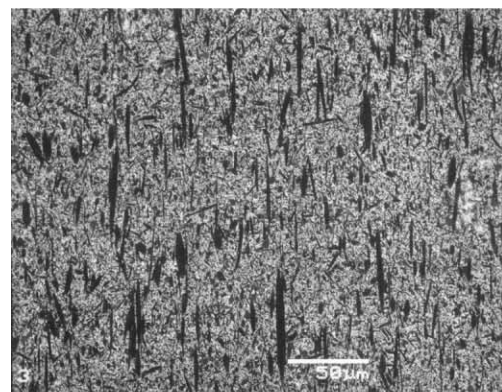
Fig. 4 shows a photograph of samples N–S–N and S–N–S. The samples were cut parallel to the casting direction, and the photograph was taken on surface L near the edge. Fig. 4 demonstrates that presence of the whisker seeds inhibits the linear shrinkage parallel to the casting direction during sintering. The middle portions



(a)



(b)



(c)

Table 1

Grain size and aspect ratio of the large elongated grains of the N and S samples (unit: μm)

Sample	Length	Width	Aspect ratio
N	5.26	2.58	5.62
S	12.67	2.82	10.53

Fig. 2. SEM micrographs of samples: (a) N, (b) N–S–N, and (c) S.

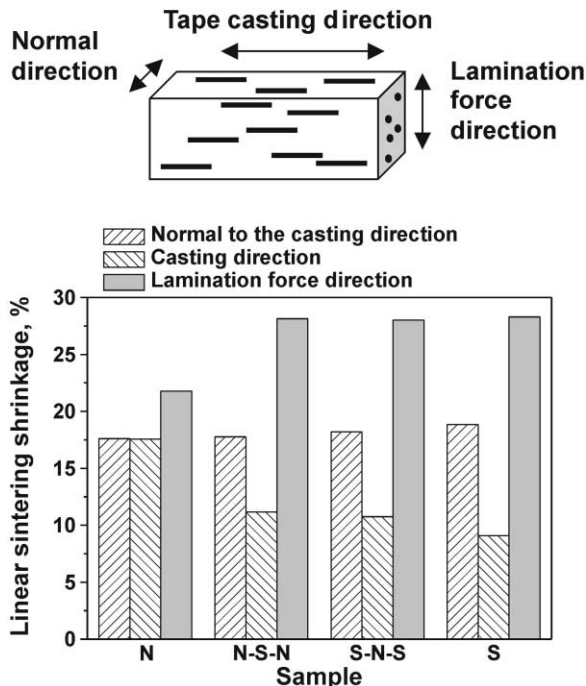


Fig. 3. The sintering shrinkage of samples in the three directions shown in Fig. 1.

of the samples were convex and concave toward the centers of the samples, respectively. There is no sharp step at the border between the layers with the whiskers and the layers without the whisker. Fig. 4 suggests that there is a strong interaction between the layers when the sintering shrinkage occurs. The shrinkage parallel to the casting direction in N layer is decreased near the border with S layer while that in the normal direction is not influenced by the presence of S layer. That results in a sintering shrinkage anisotropy in the casting plane of N layer that originally was not present. The sintering shrinkage anisotropy of N layer induced by that of S layer in contact is considered to influence upon orientations of the large elongated grains within N layer: It tends to rotate those grains parallel to the casting direction as schematically shown in Fig. 5.

Fig. 6 shows distribution of angles between the long axes of the large elongated grains and the casting direction. The wider the distribution, the more randomly oriented the grains. The angle distribution of sample N shown in Fig. 6(a) shows that the elongated grains are randomly oriented. Meanwhile, Fig. 6(b) shows that the angles are highly populated around the zero degree. It means that the large elongated grains of sample S are highly aligned in the casting direction. As a quantitative measure of degree of alignment, the average of the angles is obtained. When completely random orientations of the grains are assumed, the average angle should be 45 degrees. The smaller the angle, the better aligned the elongated grains. The average values obtained from the casting planes (surface T) of samples N and S are 42.19

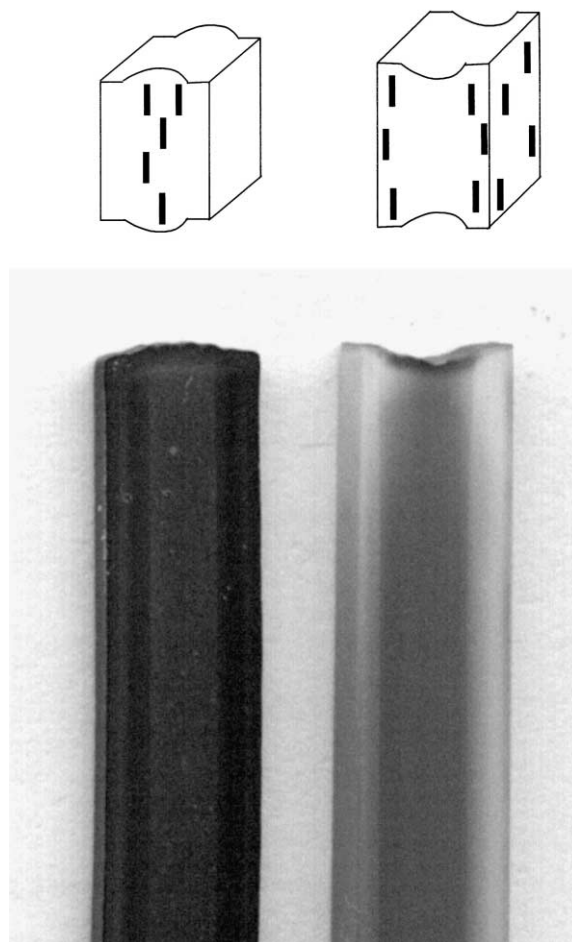


Fig. 4. Photograph of samples N-S-N (left) and S-N-S (right); samples were cut as shown in the schematic diagram.

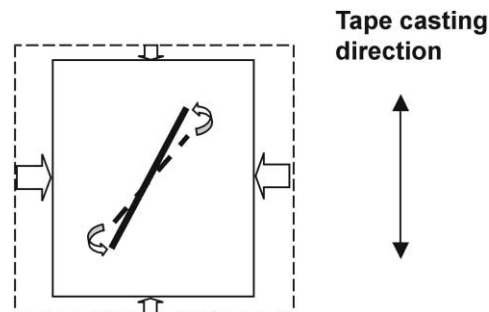


Fig. 5. Schematic diagram for alignment of large elongated grains in the N layer due to the sintering shrinkage anisotropy induced by that in the S layer; broken line, before sintering, solid line, after sintering.

degrees and 24.27 degrees, respectively. The large elongated grains growing from the whisker seeds in sample S are highly aligned. The large elongated grains in layer N of sample N-S-N are better aligned than those in sample N as shown in Fig. 6(a) and (c), and this is due to the sintering shrinkage anisotropy in N layer induced by

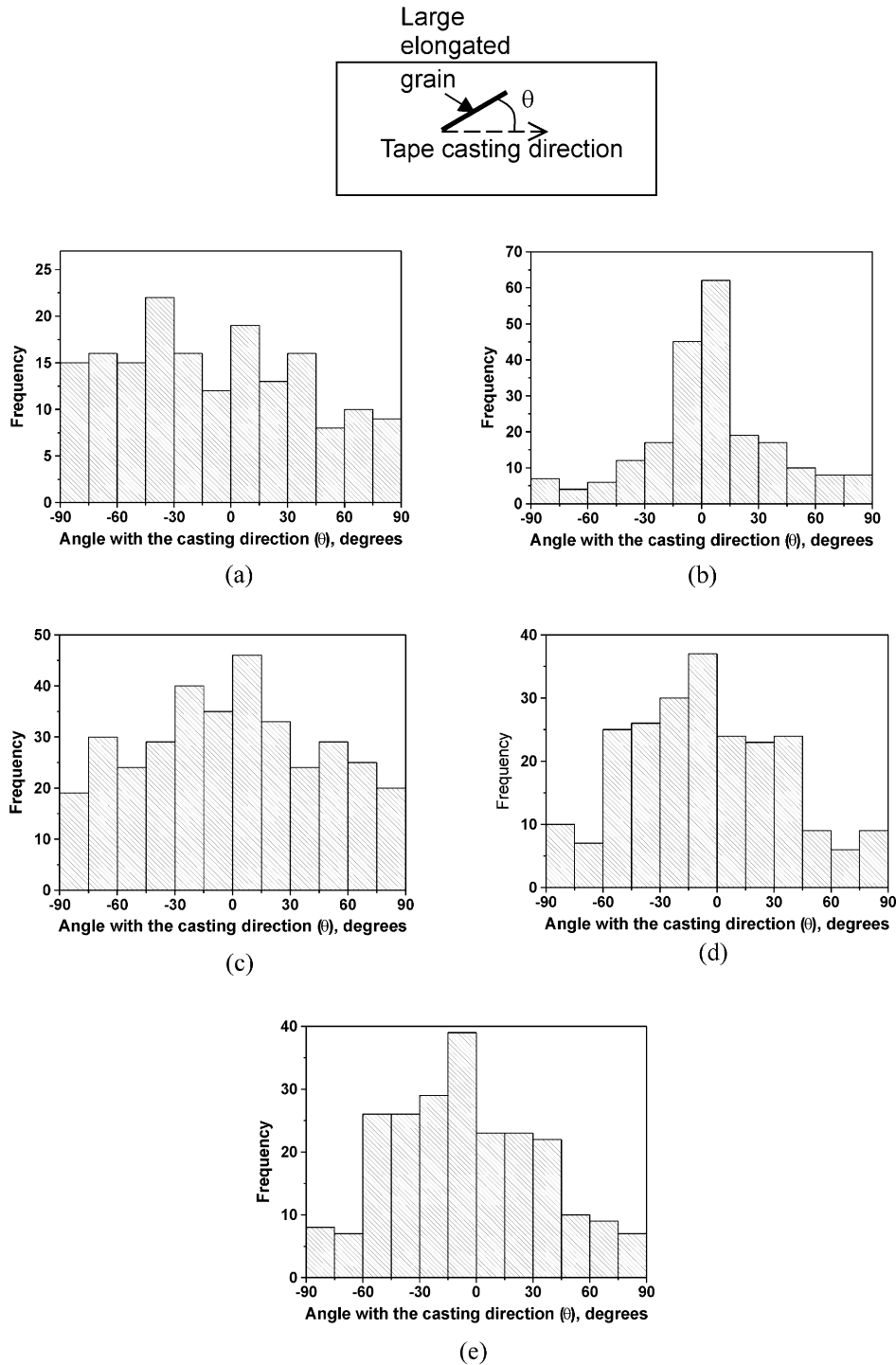


Fig. 6. Distribution of the angle between the long axes of large elongated grains and the casting direction; (a) obtained from surface T of sample N, (b) from surface T of sample S, (c) from surface T of sample N–S–N with about 0.15 mm thick surface layer, (d) from surface L of sample N, (e) from surface L of the N layer of sample N–S–N.

that in S layer as described in Fig. 5. Since the sintering shrinkage anisotropy in the N layer of the tri-laminate samples increases as it approaches the border with S layer, the degree of alignment in N layer of the sample is higher near the border than far from it. Average angle between the casting direction and the long axes of large

elongated grains on surface T of sample N–S–N with about 0.15 mm thick surface layer is 39.1 degrees. Comparison of Fig. 6(a) and (d) or Fig. 6(c) and (e) shows that the elongated grains look better-aligned on surface L than on surface T. Average angle obtained from surface L of sample N is 33.95° that is much

smaller than that obtained from surface T. The average angle obtained from surface L of N layer of sample N–S–N is 33.5° . The large elongated grains on surface L of the N layer look better aligned than those on surface T. That is in part due to smaller sintering shrinkage anisotropy on surface T than on surface L of the sample. It is also in part due to the fact that the large elongated grains normal to surface L are not considered because of the short grain length appearing on that surface.

3.2. Mechanical properties

Fig. 7 shows the three point flexural strengths of samples. Samples N and N–S–N show higher strength than samples S and S–N–S. In other words, samples with surface layer consisting of fine microstructure show higher strength than those with surface layer containing the large whisker grains. Fig. 8 shows the fracture origin of sample S that is the large elongated grain lying normal

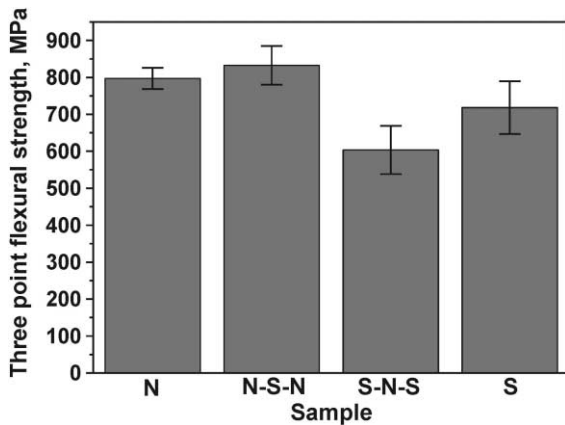


Fig. 7. The three point flexural strengths of samples.

to the casting direction. The flexural strength is influenced by the large elongated grains on the surface especially when they are oriented normal to the tensile stress. Comparison of the flexural strengths of samples N and S with those of samples N–S–N and S–N–S, respectively reveals that the strength of sample N–S–N is higher than that of sample N and sample S is stronger than sample S–N–S. In other words, samples with an S layer in the middle show higher strengths than those with an N mid-layer. It means that not only the surface layer but also the middle layer exerts an influence upon the strength of the sample. Fig. 9 shows the fracture toughness values obtained from the casting surface of the sample. Samples show anisotropic fracture toughness values except sample N; the fracture toughness is higher normal to the casting direction than parallel to the direction. In other words, the fracture toughness is higher normal to the aligned elongated grains than parallel to them. The crack propagation direction during the flexural strength measurement is normal to the aligned large elongated grains. The fracture toughness (K_{Ic}) is related to the fracture strength (σ) by

$$\sigma = \frac{K_{Ic}}{Y\sqrt{C}}, \quad (1)$$

where Y is a constant and C is the flaw size.¹⁴ For surface flaws of the same size, the fracture strength is increased as the fracture toughness is increased. Therefore, the higher flexural strengths of samples N–S–N and S than those of samples N and S–N–S, respectively are in part due to higher fracture toughness of S layer than that of N layer.

Fig. 9 also shows that the fracture toughness obtained from layer S is decreased by making the tri-laminate

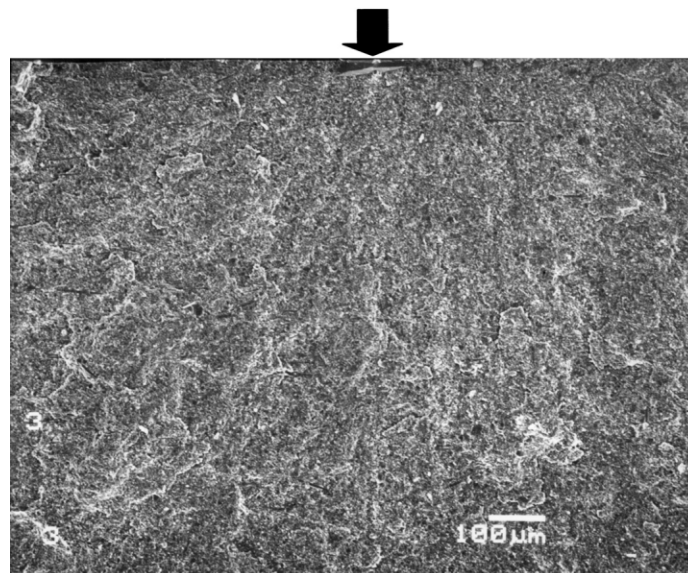


Fig. 8. SEM micrograph showing the fracture origin (indicated by arrow) of sample S.

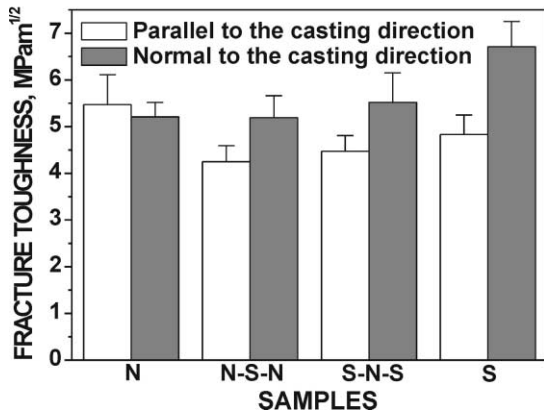


Fig. 9. Fracture toughness values of samples obtained by indentation on the casting plane; thickness of the surface layers of samples N–S–N and S–N–S was about 0.2 mm.

composites. The fracture toughness of sample N–S–N shows a value similar to that of sample N in the direction normal to the casting direction while the former sample has a lower fracture toughness than the latter sample in the casting direction. One possible explanation for these results is that the large elongated grains are slightly better aligned in sample N–S–N than in sample N, and the crack in the casting direction propagates farther along their grain boundary in the former sample than in the latter sample. In the case of sample S–N–S, the fracture toughness in the direction normal to the casting direction is lower than that of sample S. One possible explanation for the lower fracture toughness of sample S–N–S than that of sample S is that degree of alignment in the former sample is lower than that in the latter sample. The crack normal to the casting direction encounters fewer large elongated grains growing from the whisker seeds and experiences less resistance in sample S–N–S than in sample S, during its propagation. This is why the fracture toughness of sample S–N–S is lower than that of sample S in the direction normal to the casting direction.

Table 2 shows the elastic properties and the thermal expansion coefficients of the N sample and S sample. In spite of the high degree of alignment of those large

Table 2
Elastic properties and thermal expansion coefficients of the N and S samples

Sample	Young's modulus (GPa)	Poisson's ratio	Linear thermal expansion coefficient ($\times 10^{-6}/\text{K}$)
N	312	0.28	3.24
S	// ^a 302	0.29	3.33
	\perp ^b 307	0.31	3.30

^a // Parallel to the alignment direction.

^b \perp Normal to the alignment direction.

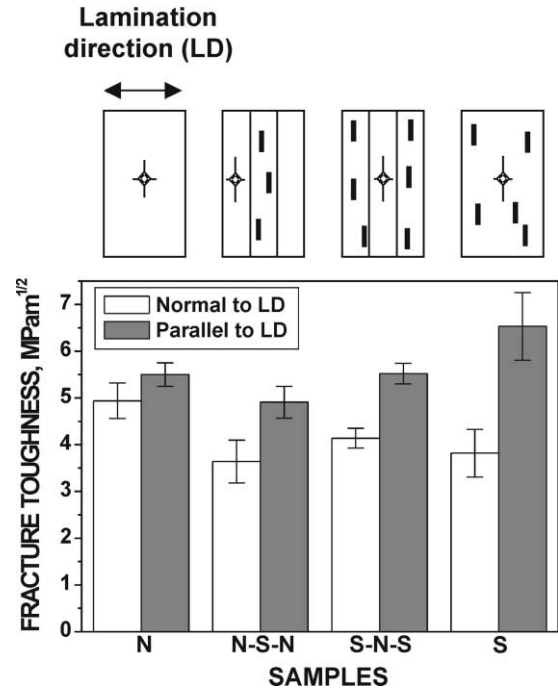


Fig. 10. Fracture toughness values obtained from surface L by indentation using 49 N load; indentation was performed on the N layer at 0.25 and 0.3 mm away from the border with the S layer for samples N–S–N and S–N–S, respectively; indentation was performed in the middle of samples N and S.

elongated grains in the S sample as shown in Fig. 2(c) and 6(b), Young's moduli and Poisson's ratios of the S sample did not vary much depending on the directions. While Young's modulus were slightly higher for the N sample than for the S sample, Poisson's ratios of the S sample were slightly bigger than Poisson's ratio of the N sample. The linear thermal expansion coefficient of the S sample in either of the two directions was bigger than that of the N sample. The thermal expansion coefficient of the S sample was slightly bigger in the alignment direction than in the direction normal to the alignment direction. However, the difference between the two thermal expansion coefficients of the S sample was negligibly small, about $3 \times 10^{-8}/\text{K}$. Therefore, the thermal residual stress can not fully explain the fracture toughness anisotropy of the N–S–N and S–N–S samples that is shown in Fig. 9.

Fig. 10 shows the fracture toughness values measured from surface L of the samples. The fracture toughness of sample N shows an anisotropy on surface L unlike that on surface T that is shown in Fig. 9. As indicated in Fig. 6, large elongated grains of sample N are randomly oriented on surface T while they show some degree of alignment on surface L. Therefore, the fracture toughness in the casting direction on surface L of sample N is lower than that parallel to the lamination force direction. It is noticeable that the fracture toughness anisotropy measured from the N layer of sample N–S–N is stronger than that of sample N. That is consistent with

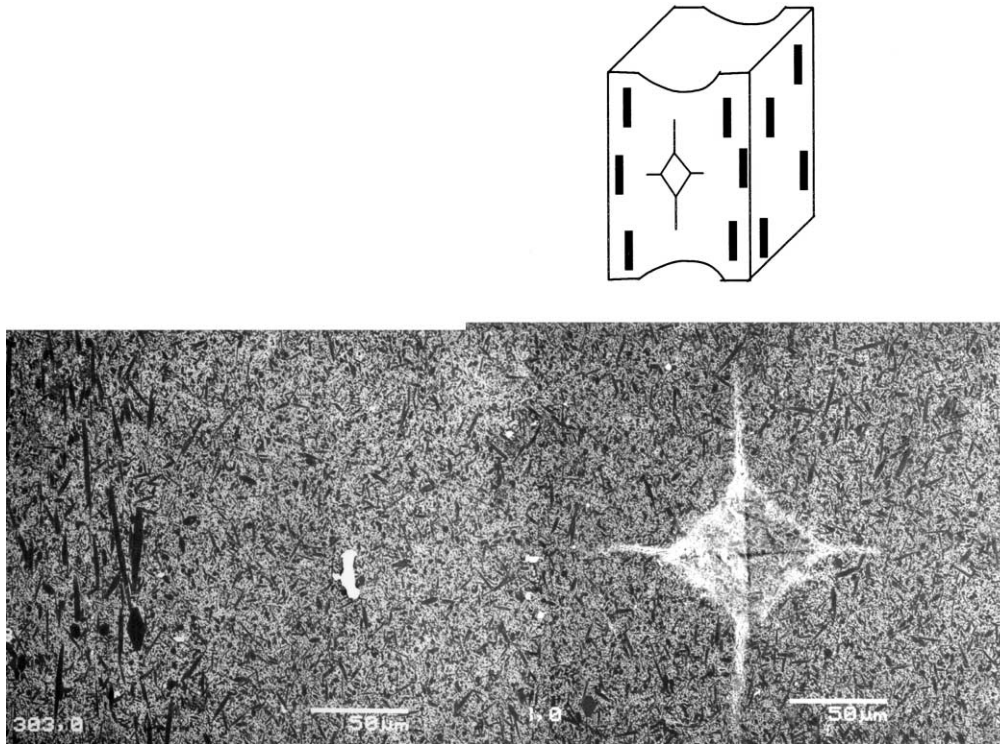


Fig. 11. SEM micrograph of indentation cracks generated in the N layer of sample S–N–S using 49 N load.

the fact that the large elongated grains in the N layer of sample N–S–N are better aligned than those of sample N as shown in Fig. 6(a) and (c). The fracture toughness values obtained from the N layer of sample S–N–S also show a strong anisotropy. The fracture toughness on surface L of sample S shows the strongest anisotropy among the samples. Fig. 11 shows SEM micrographs of the indentation cracks on surface L of the N layer of sample S–N–S. Anisotropy of the crack lengths is easily recognized and the large elongated grains in the middle layer (N layer) are oriented toward the casting direction.

4. Conclusion

Silicon nitride ceramics with laminate structures were prepared using two kinds of layers; a layer without the whisker seed and a layer with 3 wt.% whisker seeds. The sintering shrinkage was anisotropic: In case of sample N, the sintering shrinkage in the casting plane was isotropic and was smaller than the sintering shrinkage in the lamination force direction. In the case of other samples, the sintering shrinkage in the casting direction on the casting plane was the smallest, followed by that in the direction normal to the casting direction on the casting plane, and the shrinkage in lamination force direction was the biggest. In the case of samples with the tri-laminate structures, the large elongated grains in the N layer were induced to rotate toward the casting direction by the sintering shrinkage anisotropy of the S layer in contact.

The three point flexural strength depends not only on the surface layer but also on the middle layer. Samples with a N layer on the surface show higher strength than those with an S layer, while samples with an S layer in the middle show higher strength than those with an N layer. It shows that the strength is higher for the sample with higher fracture toughness when the size of the surface flaw is fixed. The fracture toughness obtained from the N layer of the samples with tri-laminate structures shows an anisotropy resulting from the microstructural anisotropy that is induced by the sintering shrinkage anisotropy of the S layer in contact.

References

1. Lee, K.-M., Lee, Y.-H., Koh, Y.-H., Choi, J.-J. and Kim, H.-E., Microstructural evolution and mechanical properties of gas-pressure-sintered Si_3N_4 with Yb_2O_3 as a sintering aid. *J. Mater. Res.*, 1999, **14**, 1904–1909.
2. Hirao, K., Ohashi, M., Brito, M. E. and Kanzaki, S., Processing strategy for producing highly anisotropic silicon nitride. *J. Am. Ceram. Soc.*, 1995, **78**, 1687–1690.
3. Gelfuso, M. V., Thomazini, D. and Eras, J. A., Synthesis and structural, ferroelectric, and piezoelectric properties of $\text{SrBi}_4\text{Ti}_4\text{O}_{15}$ ceramics. *J. Am. Ceram. Soc.*, 1999, **82**, 2368–2372.
4. Hong, S.-H. and Messing, G. L., Development of textured mullite by templated grain growth. *J. Am. Ceram. Soc.*, 1999, **82**, 867–872.
5. Sandlin, M. S. and Bowman, K. J., Textures in AlN–SiC composite ceramics. In *Materials Research Society Symposium Proceedings, Vol. 327, Covalent Ceramics II, Non-Oxides*. Material Research Society, Pittsburgh, PA, 1994, pp. 263–268.

6. Seabaugh, M. M., Hong, S. H. and Messing, G. L., Processing of textured ceramics by templated grain growth. In *Ceramic Microstructures: Control at the Atomic Level*, ed. A. P. Tomsia and A. Glaeser. Plenum Press, New York, 1998, pp. 303–310.
7. Lee, K. S., Lee, S. K., Lawn, B. R. and Kim, D. K., Contact damage and strength degradation in brittle/quasi-plastic silicon nitride bilayers. *J. Am. Ceram. Soc.*, 1998, **81**, 2394–2404.
8. Rao, M. P., Sanchez-Herencia, A. J., Beltz, G. E., McMeeking, R. M. and Lange, F. F., Laminar ceramics that exhibit a threshold strength. *Science*, 1999, **286**, 102–105.
9. Choi, B.-J., Koh, Y.-H. and Kim, H.-E., Mechanical properties of Si₃N₄-SiC three layer composite materials. *J. Am. Ceram. Soc.*, 1998, **81**(10), 2725–2728.
10. Moya, J. S., Sanchez-Herencia, J. A., Bartolome, J. F. and Tanimoto, T., Elastic modulus in rigid Al₂O₃/ZrO₂ ceramic laminates. *Script. Mater.*, 1997, **37**(7), 1095–1103.
11. Park, D.-S., Choi, M.-J., Kim, H.-D. and Han, B.-D., Orientation-dependent properties of silicon nitride with aligned reinforcing grains. *J. Mater. Res.*, 2000, **15**, 130–135.
12. Mitomo, M. and Uenosono, S., Microstructural development during gas-pressure sintering of α -silicon nitride. *J. Am. Ceram. Soc.*, 1992, **75**, 103–108.
13. Park, D.-S. and Kim, C.-W., Anisotropy of silicon nitride with aligned silicon nitride whiskers. *J. Am. Ceram. Soc.*, 1999, **82**, 780–782.
14. Hertzberg, R. W., In *Deformation and Fracture Mechanics of Engineering Materials*. John Wiley & Sons, 1976, p. 270.